Dynamics of Electron Transfer between Intercalated Polycyclic Molecules: Effect of Interspersed Bases

Anne M. Brun and Anthony Harriman*

Contribution from the Center for Fast Kinetics Research, The University of Texas at Austin, Austin, Texas 78712. *Received September 4, 1991*

Abstract: Both ethidium bromide (EB^+) and *N,N'*-dimethyl-2,7-diazapyrenium dichloride (DAP^{2+}) intercalate between base pairs in calf-thymus DNA. Upon illumination of intercalated EB^+, an electron is transferred to an adjacent intercalated DAP^{2+} molecule, as evidenced by laser flash photolysis techniques. The rate of forward electron transfer decreases with increasing number of interspersed nucleic acid bases and, for the closest approach (≈10 Å), $k_{fet} = (1.3 \pm 0.2) \times 10^9\ s^{-1}$, whereas reverse electron transfer occurs on a much longer time scale ($k_{ret} = (5.0 \pm 0.8) \times 10^7\ s^{-1}$). Similar behavior was observed with acridine orange (AO) in place of EB^+. Treating the kinetic data according to $k_{fet} = A \exp(-\beta R)$, where R is the separation distance, gave a β value of (0.88 ± 0.08) $Å^{-1}$ for both EB^+ ($A = 1.1 \times 10^{13}\ s^{-1}$; $\Delta G° = -25$ kJ mol^{-1}) and AO ($A = 2.9 \times 10^{13}\ s^{-1}$; $\Delta G° = -65$ kJ mol^{-1}). This attenuation factor is consistent with electron tunneling through the interspatial base pairs rather than via the phosphate or ribose functions.

It is well established that electron transfer in protein matrices can occur over long distances (>10 Å) at appreciable rates[1] which depend upon the tunneling pathway.[2] Similar processes may be expected to occur between weakly-coupled donor–acceptor species intercalated between base pairs in polynucleotides. In such systems, electron tunneling must proceed through the noncovalent, essentially rigid and nonpolar matrix that links donor with acceptor. *An important parameter in understanding the mechanism of DNA-mediated electron transfer, therefore, concerns the distance dependence of electronic coupling within the duplex.* As a first step toward quantifying this factor, we describe the dynamics of photoinduced electron transfer between intercalated, but seperate, donor and acceptor species, as illustrated below.

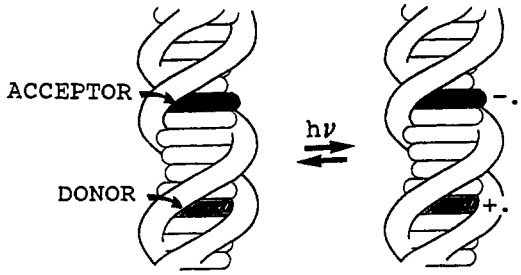

Previous studies have shown the feasibility of electron transfer between intercalated reagents,[3] between "partially" intercalated transition metal chelates,[4] and between intercalated dyes and electron acceptors bound to the outer-surface of the DNA coil.[5] However, no direct spectroscopic evidence has been presented that confirms electron transfer between properly intercalated reagents, and there is a complete scarcity of experimental data relating to reorganization energies, electronic coupling elements, and attenuation factors for electron transfer processes occurring within a polynucleotide matrix.

Experimental Section

N,N'-Dimethyl-2,7-diazapyrenium dichloride (DAP^{2+}) was prepared and purified according to the method of Hünig et al.,[6] whereas ethidium bromide (EB^+) and acridine orange (AO) were purchased from Sigma Chem. Co. and used as received. Highly-polymerized deoxyribonucleic acid, (DNA), from calf-thymus, was purchased from Sigma Chem. Co. and used as received. Stock solutions of DNA were prepared by dissolution overnight in 5 mM phosphate pH 7 buffer containing 5 mM

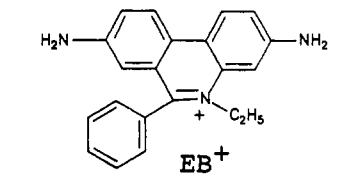

EB^+

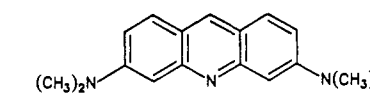

AO

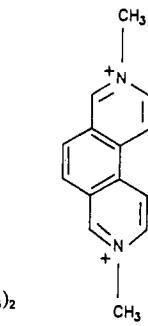

DAP^{2+}

sodium sulfate and were stored at 4 °C in the dark for short periods only. Concentrations of DNA per nucleotide phosphate were determined by absorption spectroscopy using a molar extinction coefficient of 6600 M^{-1} cm^{-1} at 260 nm.[7] Water was distilled fresh from a Millipore-Q system.

Intercalation of EB^+ or AO is accompanied by substantial red-shifts and hypochromicity of the absorption bands and by marked increases in fluorescence quantum yield and lifetime.[8] There is also a red-shift in the fluorescence spectrum. Wherever possible, excitation and monitoring wavelengths were selected so as to discriminate in favor of intercalated reagent. Intercalation of DAP^{2+} involves large red-shifts and hypochromicity of the absorption bands and a dramatic decrease in fluorescence quantum yield and lifetime.[9]

Absorption spectra were recorded with a Hitachi U3210 spectrophotometer, and fluorescence spectra were recorded with a Perkin-Elmer LS5 spectrofluorimeter, after correction for spectral responses of the instrument.[10] Fluorescence quantum yields were calculated using the optically dilute method with quinine bisulfate in 1 N H_2SO_4 as reference,[11] for which the fluorescence quantum yield was taken to be 0.55. Excited singlet state lifetimes were determined by the time-correlated, single-photon-counting technique[12] using a mode-locked Nd-YAG synchronously-pumped, cavity-dumped Rhodamine 6G or Styryl-9 dye laser. The excitation wavelength was tuned to selectively excite ethidium

(1) (a) Axup, A. W.; Albin, M.; Mayo, S. L.; Crutchley, R. J.; Gray, H. B. *J. Am. Chem. Soc.* **1988**, *110*, 435. (b) Wallin, S. A.; Stemp, E. D. A.; Everest, A. M.; Nocek, J. M.; Netzel, T. L.; Hoffman, B. M. *J. Am. Chem. Soc.* **1991**, *113*, 1842. (c) Isied, S. S.; Vassilian, A.; Wishart, J. W.; Creutz, C.; Schwarz, H.; Sutin, N. *J. Am. Chem. Soc.* **1988**, *110*, 635.

(2) (a) Beratan, D. N.; Betts, J. N.; Onuchic, J. N. *Science* **1991**, *252*, 1285. (b) Jacobs, B. A.; Mauk, M. R.; Funk, W. D.; MacGillivray, R. T. A.; Mauk, A. G.; Gray, H. B. *J. Am. Chem. Soc.* **1991**, *113*, 4390.

(3) (a) Baguley, B. C.; Le Bret, M. *Biochem.* **1984**, *23*, 937. (b) Davis, L. M.; Harvey, J. D.; Baguley, B. C. *Chem.-Biol. Interactions* **1987**, *62*, 45.

(4) (a) Barton, J. K.; Kumar, C. V.; Turro, N. J. *J. Am. Chem. Soc.* **1986**, *108*, 6391. (b) Purugganan, M. D.; Kumar, C. V.; Turro, N. J.; Barton, J. K. *Science* **1988**, *241*, 1645.

(5) (a) Fromherz, P.; Rieger, B. *J. Am. Chem. Soc.* **1986**, *108*, 5361. (b) Atherton, S. J. *Light in Biology and Medicine*; Douglas, R. H., Moan, J., Dal'Acqua, F., Eds.; Plenum: New York, 1988; Vol. 2, p 77.

(6) Hünig, S.; Gross, J.; Lier, E. F.; Quast, H. *Liebigs Ann. Chem.* **1973**, 339.

(7) Reichmann, M. E.; Rice, S. A.; Thomas, C. A.; Doty, P. *J. Am. Chem. Soc.* **1954**, *76*, 3047.

(8) Burns, V. W. F. *Arch. Biochem. Biophys.* **1967**, *183*, 420.

(9) (a) Blacker, A. J.; Jazwinski, J.; Lehn, J.-M.; Wilhelm, F. X. *J. Chem. Soc., Chem. Commun.* **1986**, 1035. (b) Brun, A. M.; Harriman, A. *J. Am. Chem. Soc.* **1991**, *113*, 8153.

(10) Argauer, R. J.; White, C. E. *Anal. Chem.* **1964**, *36*, 368.

(11) (a) Meilhuish, W. H. *J. Phys. Chem.* **1961**, *65*, 229. (b) Meech, S. R.; Phillips, D. *J. Photochem.* **1983**, *23*, 193.

(12) O'Connor, D. V.; Phillips, D. In *Time Correlated Single Photon Counting*; Academic Press: London, 1984.

0002-7863/92/1514-3656$03.00/0

bromide (λ = 575 nm) or acridine orange (λ = 425 nm), and fluorescence was separated from scattered laser light with a high radiance monochromator. Data analysis was made after deconvolution of the instrument response function (FWHM = 60 ps). Titrations were carried out by adding successive amounts of aqueous solutions of DAP^{2+} to a freshly-prepared DNA stock solution already containing a fixed concentration of EB^+ ([EB^+] = 70 μM, [DNA bases] = 1.4 mM) or AO ([AO] = 25 μM, [DNA bases] = 0.5 mM). All solutions were air-equilibrated. After deconvolution of the instrument response function, the ultimate time resolution of this instrument was ca. 30 ps, and all reported lifetimes had a reproducibility of better than ±7% of the quoted value.

Laser flash photolysis studies were made with a frequency-doubled Nd-YAG laser. For ns time scale studies, the laser was Q-switched and a pulsed Xe arc lamp was used as monitoring beam. The laser intensity was attenuated with crossed-polarizers and solutions were purged thoroughly with N_2 before and during the experiment. Solutions contained EB^+ (70 μM), DNA (1.4 mM bases), and various concentrations of DAP^{2+} (0–170 μM). Spectra were recorded point-by-point with five individual records being computer-averaged at each wavelength. Kinetic studies were made at fixed wavelengths with 50 individual records being averaged, baseline-corrected, and analyzed by computer nonlinear, least-squares iterative procedures.

Improved time-resolution was obtained with a Nd-YAG mode-locked laser operated in the pump-probe technique.[13] Approximately 300 individual shots were averaged at each time delay, baseline-corrected, and analyzed by computer iterations. This technique demands a higher absorbance at the excitation wavelength than used for fluorescence or ns laser flash photolysis studies and solutions contained EB^+ (120 μM), DNA (1.4 mM bases), and DAP^{2+} (120 μM). For AO ([AO] = 80 μM, [$DAP]^{2+}$] = 100 μM, [DNA bases] = 1.4 mM), the excitation wavelength was 417 nm accessed by Raman-shifting the frequency-tripled output from the Nd-YAG laser with deuterated cyclohexane. Transient lifetimes measured by laser flash photolysis studies were found to be reproducible to within ±10% of the quoted value. No degradation of the sample was observed during the photophysical studies.

Redox potentials for intercalated reagents were measured by cyclic voltammetry using a glassy carbon microdisc as working electrode, a Pt microdisc as counter electrode, and an SCE reference electrode. Solutions contained DNA (1.4 mM) loaded with reagent (100 μM) in water containing 5 mM phosphate buffer and 0.2 M electrolyte (NaCl or Na_2SO_4, respectively, for reduction or oxidation processes).

Results and Discussion

Fluorescence Quenching. In neutral aqueous solution (total ionic strength 30 mM) DAP^{2+} does not quench the fluorescence yield or lifetime of either EB^+ or AO with a measurable efficiency despite favorable thermodynamics for photoinduced electron transfer. The maximum concentration of DAP^{2+} that can be used for such experiments is restricted to <5 mM, because of aggregation, such that diffusional encounter between the reactants cannot compete with the inherent deactivation processes of the excited singlet state. Photoinduced electron transfer does occur between intercalated reagents, but this simply reflects a normal concentration effect that lowers the reaction volume and it should not be mistaken for a special "accelerating" effect of the polynucleotide.[4]

Intercalation of ethidium bromide (EB^+) into calf-thymus DNA (5 mM phosphate buffer pH 7 containing 5 mM Na_2SO_4) occurs with a saturation (n) of 0.5/base pair[14] and a binding constant[15] (K) of 2.6 × 10^6 M^{-1}. At [EB^+] = 70 μM and [DNA bases] = 1.4 mM, more than 99% of EB^+ is calculated to be intercalated and, assuming a nonrandom distribution, the average distance between chromophores is 10 base pairs (≈34 Å).[16] This loading, on average, positions one dye molecule for each turn of the helix and, by itself, is sufficient to cause minor disruption of the polynucleotide structure. Fluorescence from intercalated EB^+ can

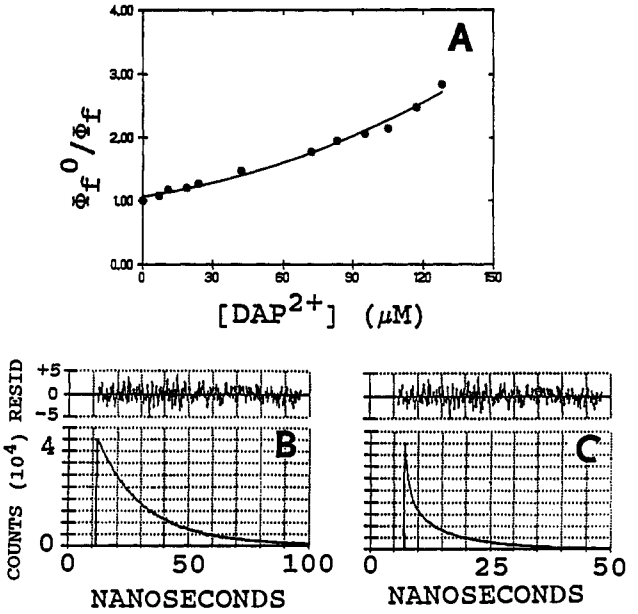

Figure 1. (A) Stern–Volmer plot for addition of DAP^{2+} to a solution of EB^+ (70 μM) intercalated into DNA (1.4 mM bases). The solid curve drawn through the data points was constructed using the integrated time-resolved fluorescence data obtained for the appropriate DAP^{2+} concentration. Time-correlated single-photon-counting decay profiles, together with weighted residuals, recorded (B) in the absence and (C) in the presence of DAP^{2+} (85 μM). Excitation wavelength was 575 nm, and fluorescence detection was at λ = 630 nm.

be detected readily[8] and decays with a lifetime (τ_0) of (21.1 ± 0.2) ns, compared to (1.6 ± 0.1) ns in water.[17] Because the absorption and fluorescence spectra characteristic of intercalated EB^+ are considerably red-shifted from those recorded for free EB^+, proper choice of excitation and emission wavelengths further discriminate in favor of intercalated dye molecules. It is possible, therefore, to make time-resolved spectroscopic measurements exclusively with the intercalated form of EB^+.

Upon addition of *N,N*-dimethyl-2,7-diazapyrenium dichloride (DAP^{2+}), which intercalates with high affinity (n = 0.25/base pair, K = 4.2 × 10^6 M^{-1}),[9] fluorescence from EB^+ was quenched (Figure 1A) and decay profiles became markedly nonexponential (Figure 1B and C). Steady-state fluorescence studies showed a progressive decrease in fluorescence quantum yield with increasing [DAP^{2+}], although Stern–Volmer plots were nonlinear (Figure 1A). Integrated decay curves and steady-state fluorescence yields exhibited very similar (i.e., ±10%) quenching levels. Indeed, as illustrated by Figure 1A it was possible to obtain a quantitative expression of the steady-state fluorescence yields by using the derived time-resolved fluorescence decay data. This finding is important because it *indicates the absence of any additional short-lived component in the decay profiles* that remained unresolved from the instrument response.

In the presence of intercalated DAP^{2+}, the complex fluorescence decay profiles could be analyzed satisfactorily[12] in terms of a three-exponential fit. Both the decay profile and the derived

$$I_f(t) = A_1 \exp(-t/\tau_1) + A_2 \exp(-t/\tau_2) + A_3 \exp(-t/\tau_3) \quad (1)$$

parameters were independent of excitation and monitoring wavelength. Analyzing the decay profiles according to various forms of "stretched" or "extended" exponentials,[18] with or without additional exponential components,[19] gave unsatisfactory analytical fits. Similarly, the decay data could not be fit to the sum of two

(13) Atherton, S. J.; Hubig, S. M.; Callen, T. J.; Duncanson, J. A.; Snowden, P. T.; Rodgers, M. A. J. *J. Phys. Chem.* **1987**, *91*, 3137.
(14) (a) Waring, M. J. *J. Mol. Biol.* **1965**, *14*, 269. (b) LePecq, J.-B.; Paoletti, C. *J. Mol. Biol.* **1967**, *27*, 87. (c) Pauluhn, J.; Zimmermann, H. W. *Ber. Bunsenges. Phys. Chem.* **1978**, *82*, 1265.
(15) Gaugain, B.; Barbet, J.; Capelle, N.; Roques, B. P.; LePecq, J.-B. *Biochemistry* **1978**, *17*, 5078.
(16) (a) Saenger, W. *Principles of Nucleic Acid Structure*; Springer-Verlag: New York, 1984. (b) Driscoll, R. J.; Youngquist, M. G.; Baldeschwieler, J. D. *Nature* **1990**, *346*, 294.
(17) Olmsted, J.; Kearns, D. R. *Biochemistry* **1977**, *16*, 3647.
(18) (a) Mataga, N. In *Molecular Dynamics in Restricted Geometries*; Klafter, J., Drake, J. M., Eds.; Wiley & Sons: New York, 1989; p 23. (b) Wallin, S. A.; Stemp, E. D. A.; Everest, A. M.; Nocek, J. M.; Netzel, T. L.; Hoffman, B. M. *J. Am. Chem. Soc.* **1991**, *113*, 1842.
(19) O'Neil, M.; Marohn, J.; McLendon, G. *J. Phys. Chem.* **1990**, *94*, 4356.

Table I. Time-Resolved Fluorescence Studies Carried out with Ethidium Bromide (70 μM) Intercalated into DNA (1.4 mM Bases) and Various Concentrations of DAP^{2+} [a]

$[DAP^{2+}]$ (μM)	τ_1 (ns)	A_1 (%)	τ_2 (ns)	A_2 (%)	τ_3 (ns)	A_3 (%)
0	21.1	100				
7	0.72	3	8.2	4	20.7	93
11	0.74	8	8.4	8	20.5	84
19	0.73	12	8.4	14	20.2	74
24	0.73	15	8.3	17	20.4	68
42	0.72	19	8.4	19	20.3	62
72	0.72	31	8.3	28	19.8	41
83	0.73	31	8.4	27	19.8	42
95	0.73	34	8.2	26	19.6	40
105	0.72	37	8.4	24	19.4	39
117	0.72	44	8.2	24	19.4	32
128	0.72	51	8.4	22	19.3	27

[a] Monochromatic excitation was made in the range 575–590 nm, where only EB^+ absorbs, and fluorescence was detected over narrow wavelength segments within the range 630–660 nm. Lifetimes and fractional amplitudes, respectively, were reproducible to within ±7% and ±12% of the quoted value.

exponentials, even at very low loadings of DAP^{2+}. The decay profiles were analyzed, therefore, according to eq 1, and the derived lifetimes (τ) and fractional amplitudes (A) are collected in Table I. This fitting procedure is biased in favor of the shorter-lived components, which can be measured with high precision but does not give an ideal representation of the decay profile at very long times. It is probable that the actual decay profile is more complex than expressed by eq 1, especially at low $[DAP^{2+}]$, but such analysis is outside our present capability.[20]

The decay profiles gave no indication of displaced EB^+, provided the concentration of DAP^{2+} was kept below ca. 120 μM,[21] although excitation and detection wavelengths were optimized in favor of preferentially observing intercalated dye. Furthermore, the fluorescence spectral records showed that added DAP^{2+} was present exclusively in the intercalated form and that, under the experimental conditions, none was bound to the polynucleotide surface or free in solution.[22] Gated fluorescence spectra, recorded at different times after the excitation pulse, were identical within experimental error and remained in excellent agreement with those recorded by steady-state methods. Inspection of the parameters extracted from our analysis of the time-resolved fluorescence decay profiles (Table I) shows that the entire titration data can be resolved into three discrete lifetimes. Thus, the lifetimes remain fixed, regardless of the amount of intercalated DAP^{2+}, as might be expected for a static system, rather than undergoing a progressive change, as might be indicative of a dynamic quenching process. This is further indication that only properly intercalated reagents are present. The two shorter lifetimes (τ_1 = (0.72 ± 0.03) ns; τ_2 = (8.4 ± 0.3) ns) increased in significance with increasing $[DAP^{2+}]$ and contributed almost equally to the total initial fluorescence intensity except at higher DAP^{2+} loadings, where the shortest lived component predominated (Table I). The longest lifetime (τ_3) remained similar to that recorded in the absence of DAP^{2+}. This value decreased systematically, in both magnitude and significance, with increasing $[DAP^{2+}]$ but appeared to reach a lower limit of (19.4 ± 0.5) ns at high loadings of DAP^{2+} (Table I).

Table II. Time-Resolved Fluorescence Studies Carried out with Acridine Orange (25 μM) Intercalated into DNA (0.5 mM Bases) and Various Concentrations of DAP^{2+} [a]

$[DAP^{2+}]$ (μM)	τ_1 (ns)	A_1 (%)	τ_2 (ns)	A_2 (%)	τ_3 (ns)	A_3 (%)
0	5.0	100				
6.4	0.25	12	2.3	14	4.7	74
8.9	0.19	17	1.9	18	4.7	65
11.0	0.20	22	1.9	22	4.6	56
17.2	0.21	35	2.1	37	4.7	28
26.5	0.21	42	2.0	30	4.5	28
31.2	0.22	45	2.1	28	4.4	27
37.4	0.22	51	2.2	24	4.4	25
41.1	0.22	54	2.1	21	4.4	25

[a] Excitation was made at 425 nm, and fluorescence was detected over narrow wavelength segments within the range 465–500 nm. Lifetimes and fractional amplitudes, respectively, were reproducible to within ±7% and ±12% of the quoted value.

Table III. Derived Rate Constants for Forward and Reverse Electron Transfer Processes Observed between Intercalated Reactants at Implied Distances (R)

	EB^+		AO
R (Å)	k_{fet} (s^{-1})	k_{ret} (s^{-1})	k_{fet} (s^{-1})
10.2	1.3×10^9	5.0×10^7	4.3×10^9
13.6	7.2×10^7	5.0×10^5	2.3×10^8
17.0	2.5×10^6	1.6×10^3	1.3×10^7

Similar time-resolved fluorescence properties were observed with acridine orange (AO) (n = 0.5/base pair, $K = 4 \times 10^5$ M^{-1})[23] in place of EB^+, and the derived values are collected in Table II. In neutral aqueous solution, AO is protonated at the aza-N atom, forming an acridinium cation,[24] and it is this species which intercalates between base pairs in DNA. Efficient fluorescence

$$AO + H^+ \rightleftharpoons AOH^+ \quad (2)$$

quenching occurs upon addition of DAP^{2+} and fluorescence decay profiles could be analyzed satisfactorily in terms of three-exponential components whose significance varied according to the $[DAP^{2+}]$. Again, alternative fitting routines failed to give a satisfactory representation of the fluorescence decay profiles.

The time-resolved fluorescence behavior is explained as follows: Intercalation of DAP^{2+} can occur at different distances from the incumbent dye molecule, incremental according to the number of interspersed base pairs, but it is quantized. The separation cannot be less than three base pairs, because of the mutual exclusion volume of the intercalated molecules, but it can be 3, 4, 5, and so on. At low loadings, there will be a statistical distribution of separation distances, allowing for any preferred binding regions, whereas a high $[DAP^{2+}]$ will raise the probability of effecting the minimum separation (i.e., three base pairs). Each intercalated DAP^{2+} molecule can quench EB^+ or AO fluorescence via an electron transfer mechanism. The rate constant for the forward

$$*EB^+ + DAP^{2+} \rightarrow EB^{2+} + DAP^+ \quad (3)$$

$$(\Delta G^\circ = -25 \text{ kJ mol}^{-1})$$

$$*AOH^+ + DAP^{2+} \rightarrow AOH^{2+} + DAP^+ \quad (4)$$

$$(\Delta G^\circ = -65 \text{ kJ mol}^{-1})$$

(20) Two points emerge from our data analysis procedures: First, having "fixed" the values for the three lifetimes by averaging the individual values derived at each separation distance, it should be possible to reanalyze the decay curves to obtain a better estimate of the fractional amplitude of each component as a function of $[DAP^{2+}]$. This information could be used in a statistical analysis to compare preference of the quencher for particular binding sites. Second, it should be possible to analyze the decay profiles in terms of a one dimensional model for electron transfer at discrete distances similar to that used to model charge transfer in random three dimensional glasses (Miller, J. R.; Beitz, J. V. *J. Chem. Phys.* **1981**, *74*, 6746). Our preliminary attempts to use such a model have been unsuccessful. We expect, however, to address both of these points in closely-related studies using synthetic intercalators.

(21) McGhee, J. D.; von Hippel, P. H. *J. Mol. Biol.* **1974**, *86*, 469.

(22) In aqueous solution, DAP^{2+} exhibits extremely intense fluorescence (Φ_f = 0.63) and possesses a long-lived excited singlet state (τ_0 = 9.0 ns). Surface-bound material is moderately fluorescent (τ = 2.7 ns), with a pronounced spectral shift from the free dye, and, consequently, very easily resolved from the nonfluorescent intercalated compound.

(23) Measured from absorption and fluorescence spectral changes in 5 mM phosphate pH buffer containing 5 mM Na_2SO_4 using the formulations expressed in ref 20.

(24) (a) Veal, J. M.; Li, Y.; Zimmerman, S. C.; Lamberson, C. R.; Cory, M.; Zon, G.; Wilson, W. D. *Biochemistry* **1990**, *29*, 10918. (b) Zimmerman, S. C.; Lamberson, C. R.; Cory, M.; Fairley, T. A. *J. Am. Chem. Soc.* **1989**, *111*, 6805.

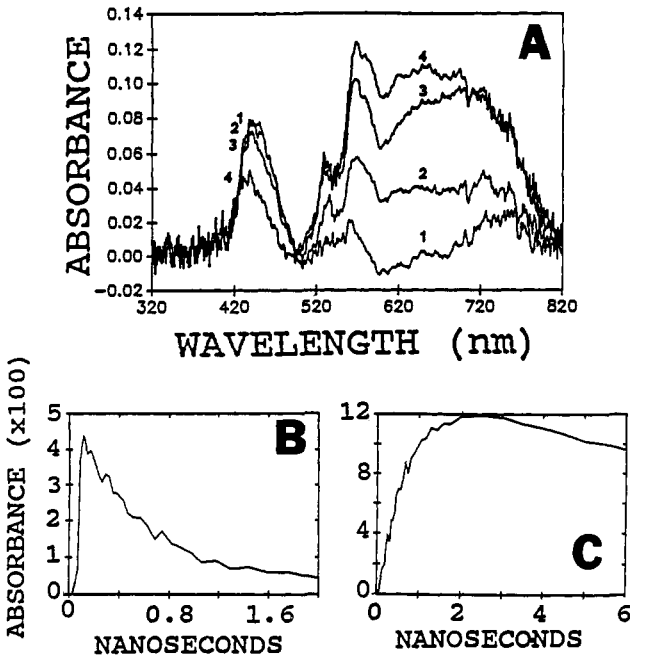

Figure 2. (A) Transient differential absorption spectra recorded after excitation of EB^+ (120 μM) and DAP^{2+} (120 μM) intercalated into DNA (1.4 mM bases) with a 30-ps laser pulse at 532 nm; delay times (1) 30, (2) 70, (3) 135, and (4) 795 ps. (B) Kinetic trace for decay of the EB^+ excited singlet state as recorded at 470 nm. (C) Kinetic trace for formation of the electron transfer products at 640 nm.

electron transfer step[25] (k_{fet}) is expected[2] to decrease with increasing reactant separation distance (R)

$$k_{fet} = A \exp[-\beta R] \quad (5)$$

where β quantifies the effectiveness of the intervening base pairs in coupling donor and acceptor species. Assuming R is quantized, τ_1 and τ_2 can be assigned, respectively, to dye molecules having a DAP^{2+} molecule separated by three (i.e., 10.2 Å) and four (i.e., 13.6 Å) base pairs. As the loading of DAP^{2+} increases, the DNA coil may unwind partially and expose the intercalated reagents to the aqueous phase[26] such that derivation of k_{fet}, at a given R, ($k_{fet} = [1/\tau - 1/\tau_0]$) is restricted to relatively low loadings. As the concentration of intercalated DAP^{2+} approaches that of the dye, few excited states will escape quenching and, under such conditions, τ_3 can be assigned to dye molecules having a DAP^{2+} molecule separated by five (i.e., 17.0 Å) base pairs. At lower loadings of DAP^{2+}, τ_3 will refer to a distribution of unquenched and quenched species and contains no useful information. Using this premise, k_{fet} can be calculated for separations of 10.2, 13.6, and 17.0 Å, assuming that the duplex remains fully coiled, and the derived values are collected in Table III. Larger separations may abound, but, in such cases, k_{fet} cannot be derived since the "quenched" and "unquenched" fluorescence lifetimes will be too similar.

Laser flash photolysis studies provided firm evidence for the formation of electron transfer products consistent with reactions 3 and 4. Thus, DNA (1.4 mM bases) was loaded with EB^+ (120 μM) and DAP^{2+} (120 μM). Immediately after excitation with a 30-ps laser pulse at 532 nm the excited singlet state of EB^+ was observed (Figure 2A).[27] This species decayed rapidly (τ_{decay} = 0.58 ns) (Figure 2B), and there was a concomitant growth (τ_{rise} = 0.64 ns) (Figure 2C) of a transient possessing the characteristic absorption spectral features of the electron transfer products

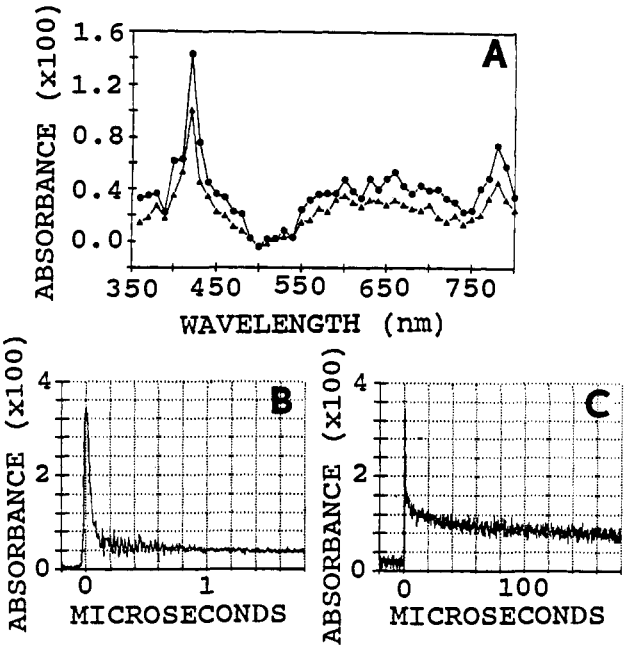

Figure 3. (A) Transient differential absorption spectra recorded after excitation of EB^+ (70 μM) and DAP^{2+} ((●) 85 μM and (○) 110 μM) intercalated into DNA (1.4 mM bases) with a 10-ns laser pulse at 532 nm. (B) and (C) kinetic traces showing decay of the electron transfer products at 640 nm.

(Figure 2A).[9,28] Under these conditions, there is a high probability of finding EB^+/DAP^{2+} couples separated by only three base pairs and the derived excited state lifetime is comparable to that observed in the time-resolved fluorescence studies (τ_1 = 0.72 ns) at much lower loadings. Electron transfer products were formed also following laser excitation of AO (80 μM) intercalated into DNA (1.4 mM) containing DAP^{2+} (100 μM) with a 30-ps laser pulse at 417 nm.[29]

Reverse Electron Transfer. Excitation of DNA (1.4 mM bases) loaded with EB^+ (70 μM) and DAP^{2+} (85 μM) with a 10-ns laser pulse at 532 nm gave rise to the electron transfer products, as monitored by transient differential absorption spectroscopy (Figure 3A). These transient species decayed via reverse electron transfer, for which $\Delta G^\circ = -187$ kJ mol^{-1}. Decay profiles were complex

$$EB^{2+} + DAP^+ \rightarrow EB^+ + DAP^{2+} \quad (6)$$

and dependent on the concentration of DAP^{2+}, although the differential absorption spectra did not change during the decay process. The shortest lived component, which dominated the decay records at high [DAP^{2+}] (Figure 3B), corresponded to a lifetime of (20 ± 3) ns. The second component had a lifetime of (2.0 ± 1.0) μs and was a relatively minor contributor to the decay profiles at high [DAP^{2+}] (Figure 3C), whereas the residual absorbance decayed slowly with a derived lifetime of (0.62 ± 0.07) ms. Lifetimes derived for the longest lived species were found to decrease with increasing intensity of the laser pulse, suggesting the involvement of bimolecular reactions. Indeed, this component may be contaminated with triplet state absorptions from unquenched EB^+ or by displaced radical cations. There was no overall degradation of the sample, even after prolonged usage of the same solution.

Effect of Separation Distance. Fitting the forward electron transfer data obtained with EB^+ to eq 5 gave a preexponential factor (A) of (1.1 ± 0.2) × 10^{13} and a β value of (0.91 ± 0.04) Å^{-1} (Figure 4). Replacing EB^+ with acridine orange (AO), for

(25) The forward and reverse electron transfer steps referred to in this study are more correctly described in terms of charge shift reactions than the more common charge separation and recombination reactions that have been studied in artificial photosynthetic model systems.

(26) Atherton, S. J.; Beaumont, P. C. *Photobiochem. Photobiophys.* **1984**, *8*, 103.

(27) Atherton, S. J.; Beaumont, P. C. *Photochem. Photobiol.* **1986**, *44*, 103.

(28) Atherton, S. J.; Beaumont, P. C. *Radiat. Phys. Chem.* **1991**, *36*, 819.

(29) Immediately after the excitation pulse the excited singlet state of AO could be observed. This species decayed with a lifetime of (0.23 ± 0.06) ns, as measured at 460 nm. There was a concomitant growth of a species absorbing in the region 550–650 nm which was assigned to the charge-separated state. This latter species did not decay within the 0–6 ns time window available with our instrument.

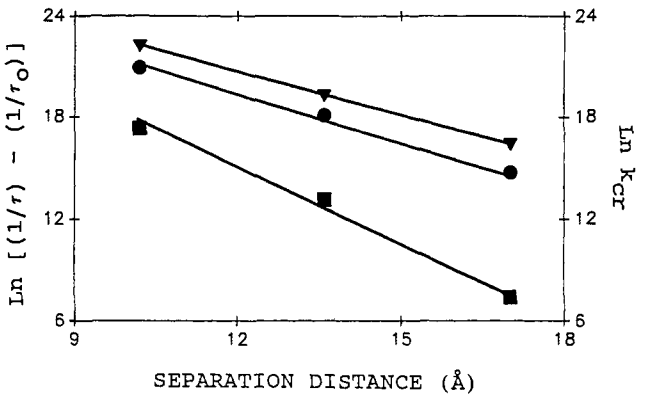

Figure 4. Correlation between the derived rate constants for forward electron transfer (k_{fet}) and separation distance (R) for EB^+ (●) and AO (▼). Data for charge recombination for the EB^+ system are included (■) also. The solid lines drawn through the data points are fits to eq 5 using the values given in the text.

which charge separation is more favorable, gave similar behavior with $A = (2.9 \pm 0.3) \times 10^{13}$ s^{-1} and $\beta = (0.86 \pm 0.04)$ $Å^{-1}$ (Figure 4). The variation in A is consistent with the changes in reaction exothermicity, whereas the average value of β [$\beta = (0.88 \pm 0.07)$ $Å^{-1}$] is comparable to values observed for modified proteins.[2] Because of the shorter distance involved, we assume that the derived β refers to electron tunneling through the intervening base pairs rather than via the phosphate or ribose functions.[2] If this is so, then electron transfer is occurring through an aromatic medium, and it is remarkable that the derived β is so similar to that found for protein residues.[2] The correspondence in β for the two systems can be used to suggest that electron transfer through a protein matrix would not occur preferentially via aromatic residues, such as tyrosine or tryptophan, but would simply follow the most direct carbon skeletal pathway.

Reverse electron transfer occurs slowly. The ps laser flash photolysis studies carried out with both systems showed no significant decay between 0 and 5 ns, whereas ns laser photolysis studies showed that the most rapid reverse electron transfer step for the EB^{2+}/DAP^+ couple has a lifetime of 20 ns. The large amount of energy that has to be dissipated during charge recombination, 187 and 157 kJ mol^{-1}, respectively, for EB^+ and AO systems, could place the process within the Marcus "inverted" region[30] and, thereby, account for the slow rates.[31] Alternately, forward and reverse electron transfer steps could occur by different routes[2] or involve different extents of electronic coupling between the reactants.[32] Recent work has demonstrated that, in certain cases, the maximum rates for forward and reverse electron transfer steps may differ considerably.[33]

Rate constants for reverse electron transfer (k_{ret}) for the EB^{2+}/DAP^+ couple (Table III) can be fit to eq 5 to give $A = (1.3 \pm 0.5) \times 10^{14}$ s^{-1} and $\beta = (1.49 \pm 0.07)$ $Å^{-1}$ (Figure 4). Such a high β value would be consistent with electron tunneling through a loosely-linked network (e.g., hydrogen-bonded),[2] whereas the derived A value is inappropriate for a reaction occurring within the "inverted" region. Indeed, in comparison to model donor–acceptor systems[34] the derived A value seems to be an order of magnitude too large.

This work has demonstrated that *long-distance (>10 Å) electron transfer processes are possible within a DNA matrix*[3-5] despite its nonpolar, rigid structure. It is noteworthy that forward electron transfer occurs with high efficiency even at modest thermodynamic driving force. Forward electron transfer appears to occur through the interspersed base pairs, and, for a photosensitizer possessing a long-lived excited state, reaction could occur over extremely long distances. This finding has important consequences for understanding the mechanism of DNA damage and repair processes. The problem associated with understanding the dynamics of reverse electron transfer demands further elaboration, and studies employing covalently-linked bis-intercalators, comprising EB^+ and DAP^{2+} subunits separated by polyamine functions, are in progress aimed at resolving this issue.

Acknowledgment. We thank Dr. Stephen J. Atherton for many helpful discussions and the National Science Foundation (CHE 9102657) for financial support. The Center for Fast Kinetics Research is supported jointly by the Biomedical Research Technology Program of the Division of Research Resources of the National Institutes of Health (RR00886) and by The University of Texas at Austin.

Registry No. EB^+, 1239-45-8; AO, 65-61-2; DAP^{2+}, 111522-98-6.

(30) Marcus, R. A. *J. Chem. Phys.* **1956**, *24*, 966.
(31) Marcus, R. A.; Sutin, N. *Biochim. Biophys. Acta* **1985**, *811*, 265.
(32) Siddarth, P.; Marcus, R. A. *J. Phys. Chem.* **1990**, *94*, 2985.
(33) Zou, C.; Miers, J. B.; Ballew, R. M.; Dlott, D. D.; Schuster, G. B. *J. Am. Chem. Soc.* **1991**, *113*, 7823.
(34) Mataga, N. In *Photochemical Energy Conversion*; Norris, J. R., Jr., Meisel, D., Eds.; Elsevier: New York, 1989; p 32.